Journal of
Molluscan Studies

The Malacological Society of London

Journal of Molluscan Studies (2021) **87**: eyab043. https://doi.org/10.1093/mollus/eyab043
Published online 21 December 2021

The shell phenotypic variability of the keyhole limpet *Fissurella latimarginata*: insights from an experimental approach using a water flow flume

Joana Vasconcelos[1,2], Diego Caamaño[3], Víctor M. Tuset[4], Ricardo Sousa[5,6] and Rodrigo Riera[1,7]

[1]*Departamento de Ecología, Facultad de Ciencias, Universidad Católica de la Santísima Concepción, Casilla 297, Concepción, Chile;*
[2]*Faculdade de Ciências da Vida, Universidade da Madeira, Campus Universitário da Penteada, Caminho da Penteada, 9020-105 Funchal, Madeira Island, Portugal;*
[3]*Departamento de Ingeniería Civil, Facultad de Ingeniería, Universidad Católica de la Santísima Concepción, Casilla 297, Concepción, Chile;*
[4]*Institute of Marine Science (CSIC), Passeig Marítim 37–49, Barcelona 08003, Cataluña, Spain;*
[5]*Direção de Serviços de Monitorização, Estudos e Investigação do Mar (DSEIMar), Direção Regional do Mar, 9000-054 Funchal, Madeira Island, Portugal;*
[6]*Observatório Oceânico da Madeira, Agência Regional para o Desenvolvimento da Investigação Tecnologia e Inovação (OOM/ARDITI), Edifício Madeira Tecnopolo, Piso 0, Caminho da Penteada, 9020-105 Funchal, Madeira Island, Portugal; and*
[7]*Grupo en Biodiversidad y Conservación, IU-ECOAQUA, Universidad de Las Palmas de Gran Canaria, Marine Scientific and Technological Park, Crta Taliarte s/n, 35214 Telde, Spain*

Correspondence: J. Vasconcelos; e-mail: joana.vasconcelos@staff.uma.pt

(Received 25 November 2020; editorial decision 11 July 2021)

ABSTRACT

Hydrodynamics are a major environmental factor on intertidal rocky shores. Morphological responses to this factor are expected to strongly influence spatial distribution of species across environmental gradients. We here analysed the shell phenotypic variability of the limpet *Fissurella latimarginata* using geometric morphometric analysis. The limpets were obtained from a sheltered intertidal coastal area and a wave-exposed environment. To determine whether the shell shape variation of the intertidal molluscs is linked to their resistance to differential intertidal wave exposure, mesocosm studies were developed in a hydraulic flume to explore the effects of hydrodynamic forces on this limpet species. A unidirectional current was used to test the impacts of step-by-step increased current flow velocities for each limpet. The phenotypic variability observed in the populations of *F. latimarginata* was associated with habitats characterized by contrasting wave exposure. Limpets from exposed environments showed a flattened, round to laterally wider and posteriorly narrower shell shape, larger foot and higher full limpet height, and were dislodged at higher velocities. A more laterally compressed and peaked shape was found in limpets from sheltered areas and these showed a lower resistance to wave action by dislodging at lower velocities.

INTRODUCTION

Rocky intertidal habitats are exposed to a greater magnitude of hydrodynamic forces (Denny & Gaines, 1990), with daily and seasonal variations that involve changes in the degree of immersion, isolation, nutrient accessibility and exposure to different levels of wave action (Newell, 1979; Truchot & Duhanel-Jouve, 1980). These spatial and temporal variations in wave action among environments (Helmuth & Hofmann, 2001; Dahlhoff, Stillman & Menge, 2002) have probably influenced the evolutionary strategies of intertidal organisms (Prowse & Pile, 2005), resulting in distinct behavioural, morphological and physiological responses (Goodrich, 1934; Trussell *et al.*, 1993; Carvajal-Rodríguez, Conde-Padín & Rolán-Alvarez, 2005; Pulgar *et al.*, 2012; Le Pennec *et al.*, 2017). The ability of a single genotype to express different phenotypes in different environments, a phenomenon known as phenotypic plasticity, is a common response to spatial variation in wave exposure (Trussell, 1997; Livore *et al.*, 2018).

The shape and size of marine molluscs may be influenced by biological processes, such as ontogenetic changes, environment adaptation or long-term evolutionary processes (Márquez *et al.*, 2015, 2018). On the intertidal shores, differences in wave energy (Etter, 1988; Trussell *et al.*, 1993), substrate type (Keough, Quinn & Bathgate, 1997; Vasconcelos *et al.*, 2020), thermal amplitude (Harley *et al.*, 2009; Livore *et al.*, 2018) and desiccation (Miller, Harley & Denny, 2009; Márquez *et al.*, 2015; Livore *et al.*, 2018) are strongly related to shape and body size, determining organisms' functional limits and species distribution boundaries across environmental gradients (Livore *et al.*, 2018). Consequently, natural selection is expected to favour traits that lower the risk of dislodgement on wave-exposed coasts (Trussell, 1997).

Mobile intertidal molluscs can resist dislodgement by (1) making use of sheltered environments, (2) having a shell shape that reduces hydrodynamic forces and (3) adhering to the substratum (Trussell *et al.*, 1993; Trussell, 1997). Thus, it has been suggested that a larger shell aperture is characteristic of wave-exposed

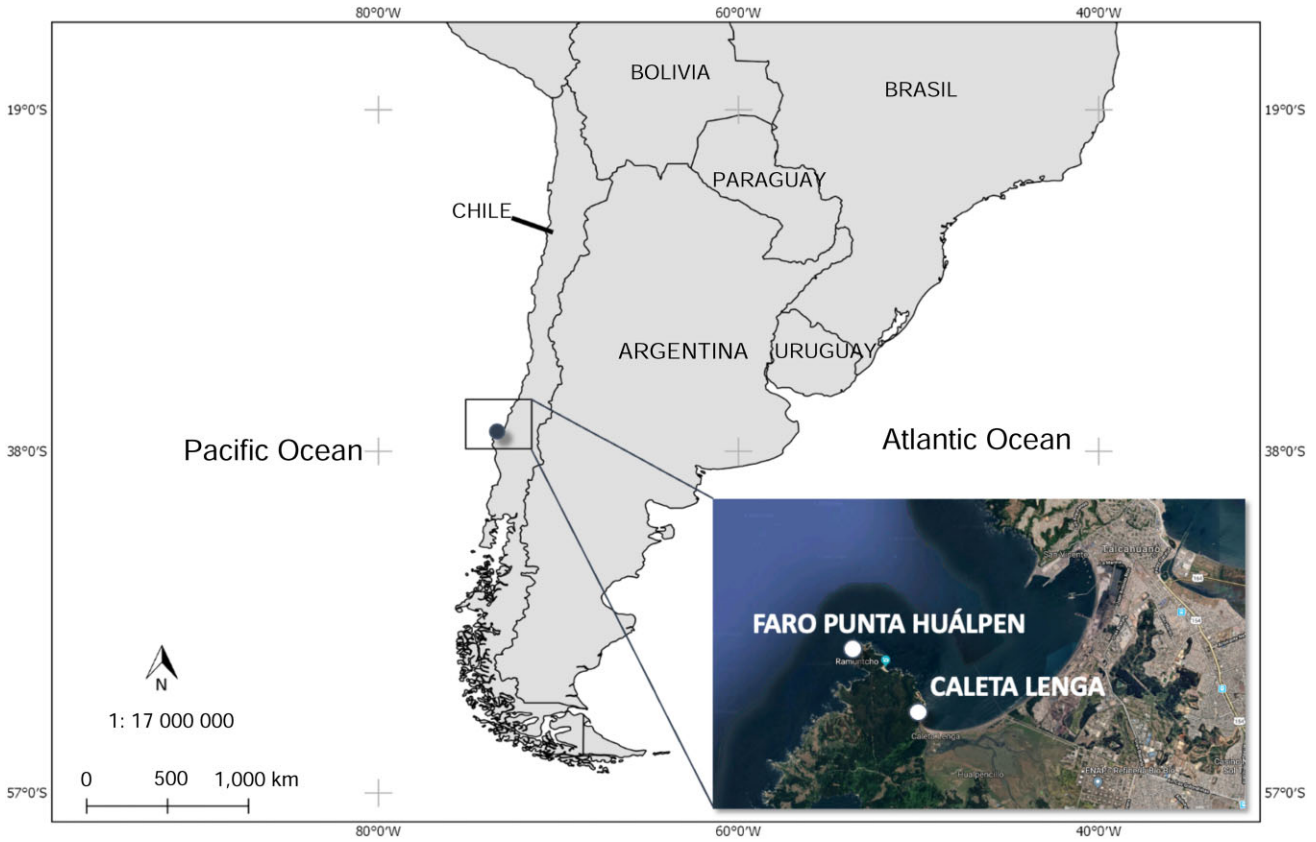

Figure 1. Map showing sampling locations of *Fissurella latimarginata* on the rocky shores of Bahía de San Vicente, Talcahuano, Chile.

environments, where the risk of dislodgement is the main selective pressure (Boulding & Van Alstyne, 1993; Queiroga *et al.*, 2011); shells become smaller and thinner with a larger aperture accommodating a larger foot, allowing increased adhesion to the rock, an essential feature for species inhabiting environments with strong wave exposure (De Wolf *et al.*, 1997). The larger the foot area, the more resistance to dislodgement due to the waves (Etter, 1988; Trussell *et al.*, 1993; Le Pennec *et al.*, 2017). Differences in size and aperture area also affects vulnerability to thermal stress and desiccation, and variation in these morphological traits may be associated with adjustments to wind and wave exposure across microhabitats (Atkinson & Newbury, 1984). Although trait–environment correlation may suggest a link, experimental data are needed to determine whether a phenotype is truly responding to variation in a specific selection pressure (Le Pennec *et al.*, 2017).

We here focus on a mollusc that has been extensively exploited in the intertidal and shallow subtidal seabeds of Chile, the keyhole limpet *Fissurella latimarginata* G.B. Sowerby I, 1835. The limpets of the genus *Fissurella* (Vetigastropoda: Fissurellidae) are considered keystone species in coastal marine ecosystems. In Chile, they play a pivotal role in the community structure of rocky shores (Oliva & Castilla, 1986) and form the basis of an artisanal fishery, having formed part of the human diet since prehistoric times (Bretos, 1988). These molluscs are under intense human pressure along the Chilean coast and this is especially so in north and central Chile (Rivadeneira, Santoro & Marquet, 2010). Due to their specialized life history traits, limited habitat and the impact of human activity on limpet habitats, these intertidal grazers are vulnerable to environmental changes (Nakin & McQuaid, 2014). We hypothesize that populations of *F. latimarginata* might show phenotypic variability in relation to environment, with dorsal and lateral shell shape and body morphometry varying with respect to the type of environment (i.e. exposed *vs* sheltered habitats), such that shell morphology reflects differing levels of resistance to different hydrodynamic regimes. Our expectation is that larger shell apertures allow a larger area of foot to be extended out of the shell; this is an important feature to avoid dislodgement by resistance to higher current velocities in exposed environments. The main goals of the present study are (1) to explore phenotypic variability in the shell shape of *F. latimarginata* in relation to the environment where specimens were caught and (2) to test experimentally whether the morphological characters shown to be linked to the type of environment influence the capacity of limpets to resist differential flow velocities.

MATERIAL AND METHODS

Data collection

Between April and July of 2019, a total of 140 specimens of *Fissurella latimarginata* were collected from the rocky shores of Bahía de San Vicente, Talcahuano, central Chile. The sample included a wide range of shell sizes and the habitats sampled were characterized by different levels of wave exposure, ranging from highly exposed habitats (near Faro Punta Huálpen; 36°44′58.754″S, 73°11′37.217″W) to sheltered ones (Caleta Lenga; 36°45′46.372″S, 73°10′30.792″W) (Fig. 1). Individuals were transported to the UCSC-Chile Marine Biology Station of Lenga and maintained in recirculating seawater tanks (open ocean water-circuit system) until they were transported to the hydraulic laboratory to assess their performance in the flume experiments (i.e. occurred within 24 h).

Morphometry and shape

Individuals were measured for total shell length (L_s; mm), shell width (W_s; mm) and full limpet height (foot + shell; H_l; mm) using

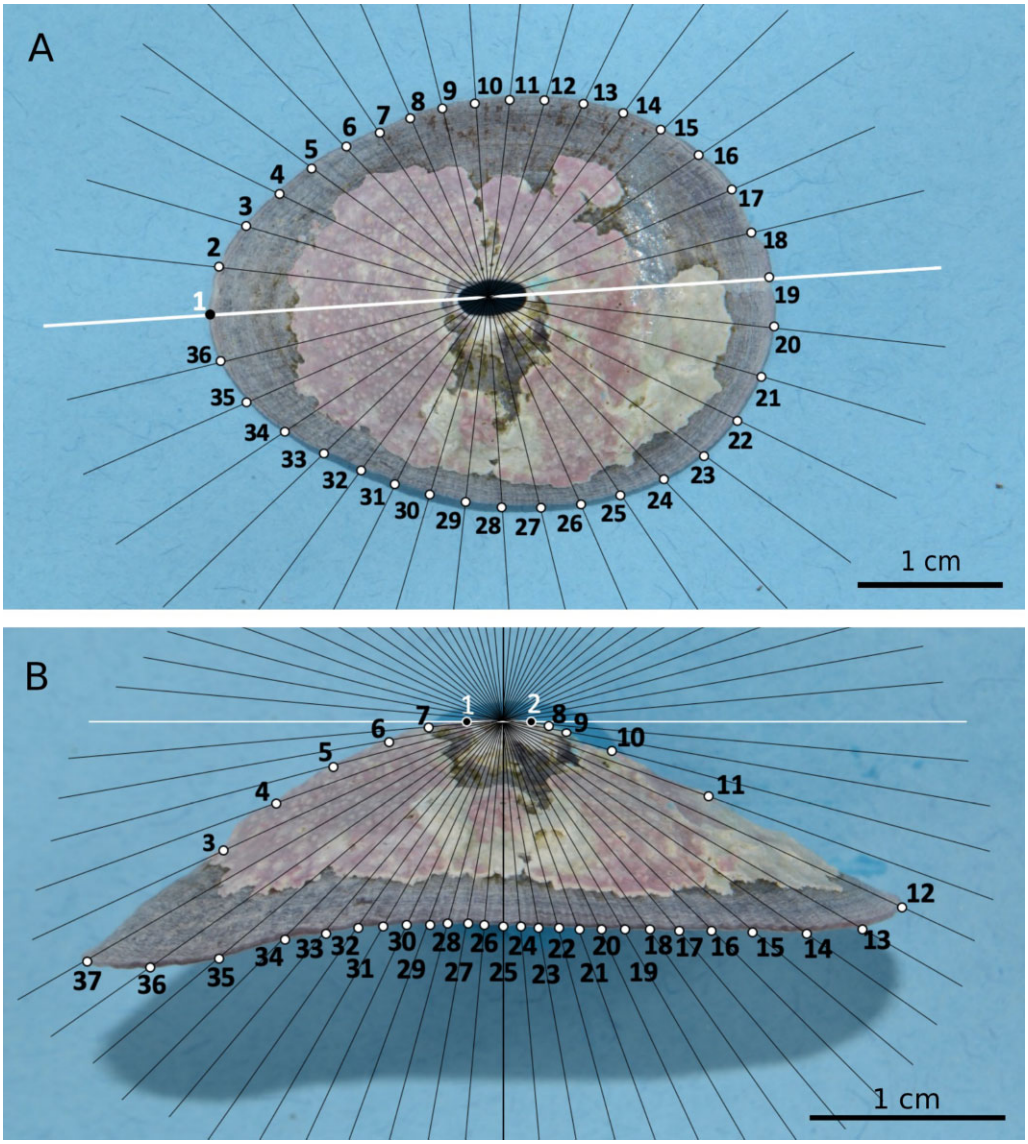

Figure 2. Schemes for dorsal (**A**) and lateral (**B**) shell shape data collection from *Fissurella latimarginata*, with black circles indicating landmarks and white circles indicating semilandmarks. In the dorsal view (**A**), LM1 was identified on the anterior border of the axis that corresponds to the greatest total shell length. A system of axes equally distant in 10° was used to obtain 35 semilandmarks and these were placed on the intersection of the fan and the shell border of each sample specimen. In the lateral view (**B**), LM1 and LM2 were placed on the shell apex of each limpet and a fan composed of a system of axes equally distant in 5° was superimposed to determine the position of 35 semilandmarks.

a calliper (0.01 mm) (Supplementary Material Fig. S1). Additionally, using ImageJ v. 1.53 (Schneider, Rasband & Eliceiri, 2012), we imaged the underside of the foot of each limpet while it was crawling on a transparent surface to estimate the limpet's foot length (L_f; mm), foot width (W_f; mm) and foot area (A_f; mm^2) (Supplementary Material Fig. S1). A Pearson's correlation was applied to determine the strength of the relationship between pairs of the continuous variables L_s, W_s, H_l, L_f, W_f and A_f. As a strong correlation was found between L_s and all the other variables (see the section on morphometry and shape in the 'Results' section), the effect of size was removed through a normalization technique used to scale data exhibiting an allometric growth (Lleonart, Salat & Torres, 2000). All individuals were scaled and their shape adjusted to the shape they would have in the new allometric size (Lleonart *et al.*, 2000):

$$Y_i^* = Y_i \left[\frac{X_0}{X_i}\right]^b, \quad (1)$$

where Y_i^* is the theoretical value of Y if the limpet length were X_0, X_i is the body length of the individual i, X_0 is the reference body length (mean X) and b is the allometric parameter relating the dependent variable Y_i with the independent variable X ($Y = aX^b$) (Lombarte & Lleonart 1993; Lleonart *et al.*, 2000). Equation (1) converts any observed point (X_i, Y_i) into a theoretical point (X_0, Y_i^*) in such a way that all observations taken at different values of X_i are normalized to a unique X_0, maintaining the particular shape factor for every individual (Lleonart *et al.*, 2000). Normality of the distribution of the normalized variables was verified through the Shapiro–Wilk normality test. Variations in normalized variables between habitats with differences in wave exposure were tested through a two-sample *t*-test (Zar, 1996).

For shape analysis, each shell was photographed for dorsal and lateral surfaces using a standardized and homologous shell position for all specimens to avoid differences in the nature of the anatomical structures between specimens. Imaging was performed using a Canon EOS 5DS R digital camera with a Canon EF 35 mm *f*/1.4L

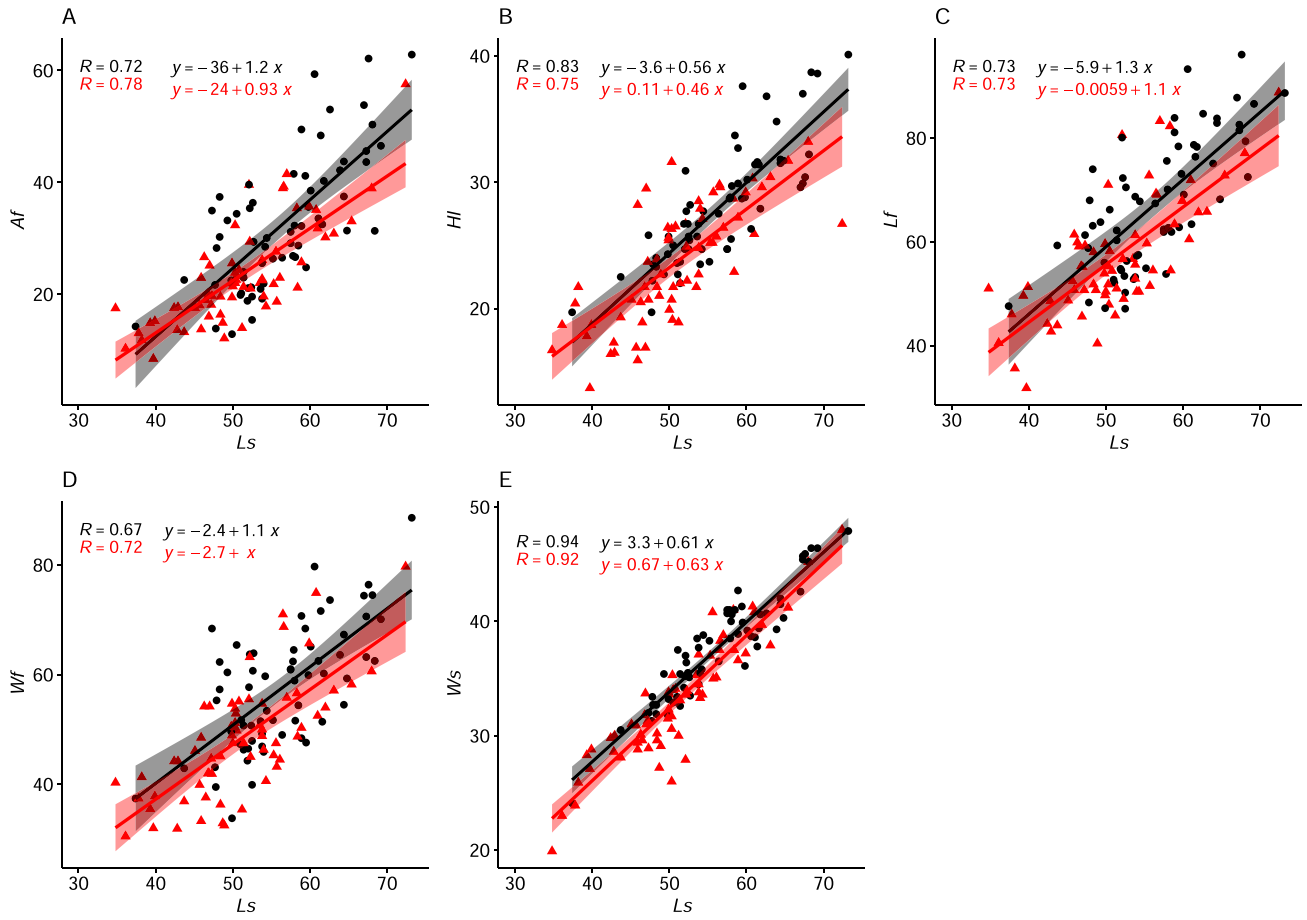

Figure 3. Scatterplot displaying the strength, direction and form of the relationship between total shell length (L_s) and the variables foot area (A_f) (**A**), full limpet height (H_l) (**B**), foot length (L_f) (**C**), foot width (W_f) (**D**) and shell width (W_s) (**E**) for shores with differential exposure to wave action. Exposed conditions are indicated by black circles and sheltered environments by red triangles.

II USM lens mounted on a Manfrotto tripod MT055XPRO3 to maintain the same distance for all samples, thus ensuring the right angle and the adequate height to stabilize and avoid image distortion. In the dorsal view, the anterior–posterior axis along the largest total shell length distance of each specimen was identified and landmark 1 identified as the most distant point of the anterior margin on the border of the shell (Fig. 2A). Then, a fan composed of a system of axes equally distant in 10° was used to position each specimen along such an axis and to ensure that the hole in the apex of each shell coincided with the horizontal line of the fan (Fig. 2A). A tps file for each specimen was created using tpsUtil v. 1.69 (Rohlf, 2017c) and the tpsDig2 v. 2.30 (Rohlf, 2017a) software was used to acquire *x* and *y* coordinates for 1 landmark and 35 semilandmarks placed on the intersection of the fan and shell of each sample specimen image. All points (at the shell border) do not necessarily represent homologous landmarks from a development point of view but can be used to objectively decompose the shell shape of limpets (Faria *et al.*, 2017). These points are referred to as semilandmarks and can be used to capture information about curvature (Gunz & Mitteroecker, 2013). For the lateral shape analysis, two landmarks (LM1 and LM2) were placed on the apex of the shell (homologous in all individuals in the analysis) and the line drawn connecting these two points served as the basis for the identification of the semilandmarks. Each shell was then superimposed onto a fan composed of a system of axes equally distant in 5° and centred to the middle point of LM1 and LM2 (Fig. 2B). This system allowed the collection through tpsDig2 of 37 landmarks and semilandmarks for each shell (2 landmarks located on the shell apex and the remaining semilandmarks located all along the shell border). For both the dorsal and lateral analyses of the shell, the pictures were individually scaled.

To remove the effect of the distortions in the position, orientation and size (Angeles *et al.*, 2014) of the landmark coordinates, a generalized Procrustes analysis (Rohlf & Slice, 1990; Rohlf, 1999) was used to adjust the landmarks and eliminate differences. This way, the configurations of the landmarks are centred, standardized (configuration of the landmarks scaled to unit centroid size) and rotated to minimize the Procrustes distances between homologous landmarks (Rohlf & Slice, 1990). To calculate and eliminate the effect of total shell length on shape (allometry), a multivariate (total) regression of the Procrustes coordinates on centroid size was carried out and the residuals of this regression were used as 'size-free' variables (Klingenberg, 2016). To assess whether shapes differ among environments, a multivariate analysis of variance (MANOVA) with 1,000 random permutations of the residuals among groups for significance testing was applied. Then, relative warp analysis of superimposed images was conducted using tpsRelw v. 1.67 (Rohlf, 2017b). Each relative warp axis represents a set of specific morphological characteristics, allowing specific morphological attributes of species to be analysed directly (Rohlf & Marcus, 1993; Farré *et al.*, 2016). A principal component analysis (PCA) on the covariance matrix of the 'size-free' Procrustes was conducted to quantify the variance of the warps explained by the PC axes (Rohlf & Marcus, 1993; Mitteroecker & Bookstein, 2011). Thin-plate spline deformation grids showing shape variation along the PC axes were implemented (Bookstein, 1997). The PCs that

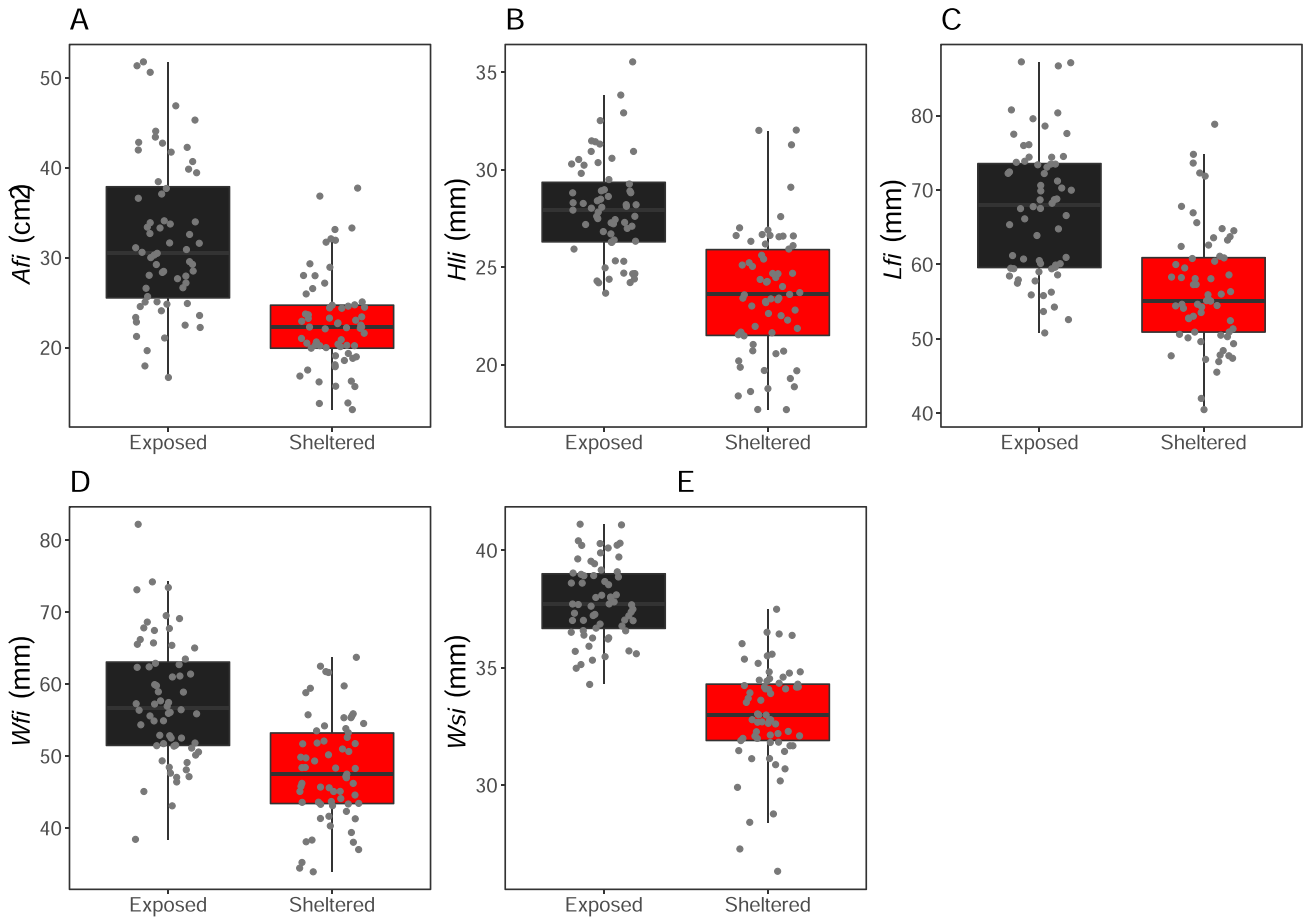

Figure 4. Variation in the five normalized variables for *Fissurella latimarginata* from shores differentially exposed to wave action. **A.** Foot area (A_{fi}). **B.** Full limpet height (H_{li}). **C.** Foot length (L_{fi}). **D.** Foot width (W_{fi}). **E.** Shell width (W_{si}). Exposed habitats are indicated by black shading and sheltered environments by red shading, with the horizontal lines within the boxes indicating the median. The dots represent the original data points.

cumulatively accounted for up to 95% of the total variation were retained (Collar & Wainwright, 2009). Canonical variate analysis (CVA) was carried out on the reduced PCA matrix to summarize the variation between factors maximizing their distances (Mardia, Kent & Bibby, 1979; Tuset *et al.*, 2016). Leave-one-out cross-validation procedure was then applied to quantify the correct classification (Lachenbruch & Mickey, 1968). The bias of the classification was determined with the Cohen's kappa coefficient, which estimates the improvement over chance of corrected classification rates (Tuset *et al.*, 2003). All analyses and graphical representation were carried out in the R packages geomorph v. 3.0.7 (Adams, Collyer & Kaliontzopoulou, 2018) and morpho v. 2.7 (Schlager, 2017) in R v. 3.5.2 (R Core Team, 2018); the thin spline illustrations were obtained using PAST v. 3.12 (Hammer, Harper & Ryan, 2001).

Laboratory-controlled water flow experiments

To test whether the geometric characteristics of limpet shells influence their capacity to resist differential flow velocities, a water flume experiment was set up. For the laboratory-controlled water flow experiments, limpets were first examined for evidence of damage (e.g. chipped shells and failure to adhere to the substrate) and only robust, undamaged individuals that could withstand attempts to remove them by hand from the substrate were retained for the flume trials. These were then tagged with nail polish, placed in a unidirectional current provided by a 5 m long, 0.32 m wide and 0.8 m deep flume (see Supplementary Material Fig. S2). Individuals were acclimatized to a gentle water flow allowing them to firmly attach to the substrate. The flow current flume was used to test the impacts of step-by-step increased water speed on *F. latimarginata* collected from both types of habitats (sheltered *vs* exposed). About 1,700 l of seawater was transported from the Marine Biology Station of Lenga to fill two high-speed flume tanks. Flow was generated using a pump mounted at one end of the flume and controlled by an adjustable speed drive (Dayton Electronic, model 6K119).

Other aspects of the experimental procedure were adapted from Le Pennec *et al.* (2017). Five maximum free-stream velocities were measured and calibrated in the central part (to minimize channel edge effect) at about three-fourths of the flume length using a Vectrino acoustic Doppler velocimeter (Nortek, Rud, Norway): (1) 1.48 m s^{-1}, (2) 1.67 m s^{-1}, (3) 2.05 m s^{-1}, (4) 2.39 m s^{-1} and (5) 2.44 m s^{-1}. These selected velocities may not attain the maximal speeds that can occur in field conditions but cover a wide range of typical water speed velocities, as they are much higher than those refereed in the works of Aguirre, Garreaud & Rutllant (2014) along south-central Chile (27–42°S; speeds in the 15–25 cm s^{-1} range) and Strub *et al.* (2019) along the southern Chile transition region (38–46°S; speeds of *c.* 5–8 cm s^{-1}).

Specimens were placed in the central part and at three-fourths of the flume length and their spacing was estimated and tested to avoid turbulence interference and physical interaction between the specimens. A maximum of five specimens per trial ensured that each individual shell was being forced by parallel flow. Each group of five specimens faced a series of three flushes with the lowest free-stream velocity (1.48 m s^{-1}) and each flush lasting 20 s, with 30 s resting time between each series. Limpets remaining in the flume

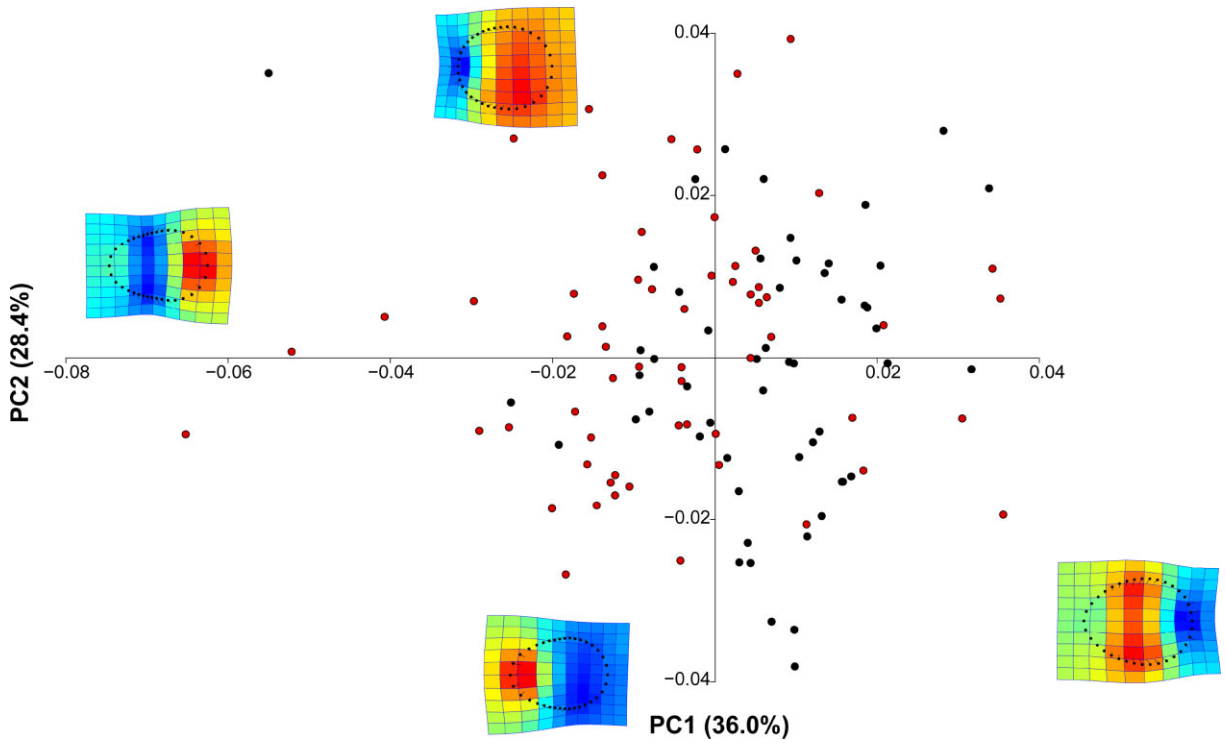

Figure 5. Plot showing PCA of Procrustes coordinates for the dorsal view of *Fissurella latimarginata* based on PC1 and PC2. Black dots indicate specimens from exposed environments and red dots indicate samples from sheltered habitats. The thin-plate spline deformation grids display shell shape, which ranges from an expanded shape (red) to a contracted one (blue); shell outlines are oriented so that the anterior portion of the shell lies on the left.

(i.e. those that were not dislodged in the first set of flushes) faced the next level of speed of the subsequent three flushes until all individuals either were dislodged or had resisted the maximum free-stream velocity of 2.44 m s^{-1}. Each individual went through this procedure three times with an increase in the duration of each flush (20, 40 and 60 s, respectively) but maintaining the 30 s resting time between each flush. Limpets that did not attach during the acclimatization period in the flume were removed from the analysis; this happened with around 7% of individuals (four from sheltered environments and six from exposed habitats).

Dimensional analysis, based on the geometric variables of the limpet and experimental fluid and flow properties, was used, and the flow velocity at which a limpet detaches (u_d) is proposed to be a function of the following variables:

$$u_d = af(v, H_d, A_f, L_f, W_f, H_l, L_s, W_s),$$

where u_d is the velocity (m s^{-1}) of flow at which the limpet is detached, a is a dimensionless constant, v is the kinematic viscosity of seawater considered constant between experiments (0.946 × 10^{-6} m^2 s^{-1}), H_d is the height (m) of flow at which the limpet is removed, A_f is the limpet's foot area (mm^2), L_f and W_f are the length (mm) and width (mm) of the limpet foot, H_l is the full height (mm) of the limpet, and L_s and W_s are the length (mm) and width (mm) of the limpet shell. The dimensionless parameter a was included to verify the relation between the geometric characteristics of the limpet and the fluid and flow properties with the velocity. If the detachment velocity shows a strong correlation with the geometric variables, then the value of a should be constant, meaning that limpet geometry, and fluid and flow properties are capable of predicting the detachment scenarios. In contrast, a nonconstant value of a suggests the presence of a source of forcing other than those relating to limpet geometry, fluid or flow (e.g. internal limpet attachment forces, such as foot strength). Thus, the subsequent velocity formulation is given by equation (2):

$$u_d = a\,v\left(\frac{1}{H_d}\right)\left(\frac{A_f}{L_f W_f}\right)\left(\frac{H_l^2}{L_s W_s}\right). \quad (2)$$

Variations in the normalized variables and in the constant a between environments with differences in wave exposure were tested per maximal velocity resisted by a two-sample t-test.

RESULTS

Morphometry and shape

The variable L_s was strongly related to the variables W_s [exposed (Exp.): $r = 0.94$; sheltered (Shl.): $r = 0.92$], H_l (Exp.: $r = 0.83$; Shl.: $r = 0.75$), L_f (Exp.: $r = 0.73$; Shl.: $r = 0.73$), W_f (Exp.: $r = 0.67$; Shl.: $r = 0.72$) and A_f (Exp.: $r = 0.72$; Shl.: $r = 0.78$) regardless of the type of environment (Fig. 3). The normalized variables W_{si}, H_{li}, L_{fi}, W_{fi} and A_{fi} obtained after removing the effect of size showed a normal distribution ($P > 0.05$; Supplementary Table S1). The morphological normalized traits W_{si} ($t_{119.13} = 14.498$, $P < 0.001$), H_{li} ($t_{120.95} = 8.4674$, $P < 0.001$), A_{fi} ($t_{105.97} = 7.4895$, $P < 0.001$), L_{fi} ($t_{124.68} = 7.2945$, $P < 0.001$) and W_{fi} ($t_{122.7} = 6.9208$, $P < 0.001$) increased towards the wave-exposed habitats (Fig. 4).

Dorsal shape analysis

The MANOVA analysis of the dorsal view of the shell revealed significant differences in shape in relation to wave exposure environment ($F = 6.025$, $P = 0.001$) but not sex ($F = 1.412$, $P = 0.245$), free-stream velocity ($F = 1.329$, $P = 0.243$) or centroid size ($F = 1.132$, $P = 0.324$).

A total of four PCs explained 91.4% of variance (see Supplementary Material Table S1). The first two PC axes explained 36% and 28.4% of total variance, respectively (Fig. 5). The thin-plate spline deformation grids for the dorsal view indicate that shell shape

Table 1. Results of the interspecific classification of the dorsal and lateral views of the shells of *Fissurella latimarginata* based on environmental factors and sex and using canonical variate analysis.

View	Factor/actual group	Predicted group membership (%)		Corrected classification (%)	Cohen's kappa
		A	B		
Dorsal	Wave exposed (A)	**68.52**	31.48	68.42	0.368
	Sheltered (B)	31.67	**68.33**		
Lateral	Wave exposed (A)	**56.10**	43.86	56.90	0.138
	Sheltered (B)	42.37	**57.63**		
	Sex				
	Females (A)	**85.08**	14.93	60.34	0.125
	Males (B)	73.47	**26.53**		

In bold, the assignation percentage for correctly predicted group membership.

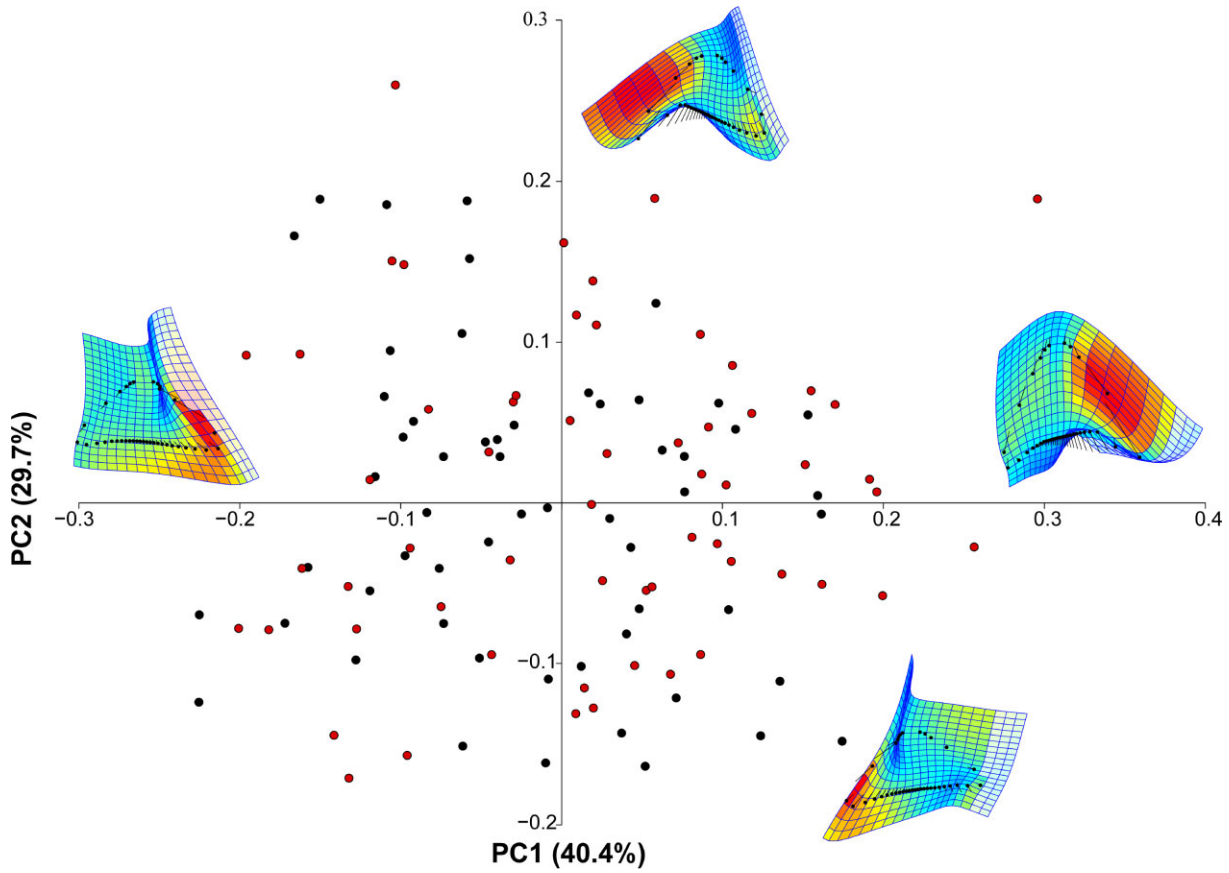

Figure 6. Plot of the PCA of Procrustes coordinates for the lateral view of *Fissurella latimarginata* based on PC1 and PC2. Black dots indicate samples from exposed environments and red dots indicate specimens from sheltered habitats. The thin-plate spline deformation grids display shell shape, which ranges from an expanded shape (red) to a contracted one (blue); shell outlines are oriented so that the anterior portion of the shell lies on the left.

changes from a more laterally compressed and posteriorly rounded shape to a laterally wider and posteriorly narrower one along PC1 (i.e. from left to right in Fig. 5). Specimens from sheltered environments tend to have negative PC1 scores, whereas specimens from exposed sites are characterized by positive PC1 scores. Positive PC2 scores are correlated with shells showing a more rounded shape, while negative PC2 scores are characteristic of shells with an oval shape. The overall assignment of *Fissurella latimarginata* individuals in their original sample was correctly classified for 68.4% of the total number of specimens, with the rate of misclassification being 31.6% (Table 1). Cohen's kappa was 0.368, indicating that classification efficiency was 36.8% better than would have occurred by chance alone (Table 1).

Lateral shape analysis

Since a significant relationship was noted between shape and centroid size ($R^2 = 0.884$, $P < 0.001$, permutations = 1,000), the residuals of the regression between them were treated as 'size-free' Procrustes for the subsequent analysis. The MANOVA analysis showed significant differences in lateral shell shape with respect to environments ($F = 2.896$, $P = 0.024$) and sex ($F = 2.782$, $P = 0.034$). PC1 explained 40.4% of total variance and revealed a high

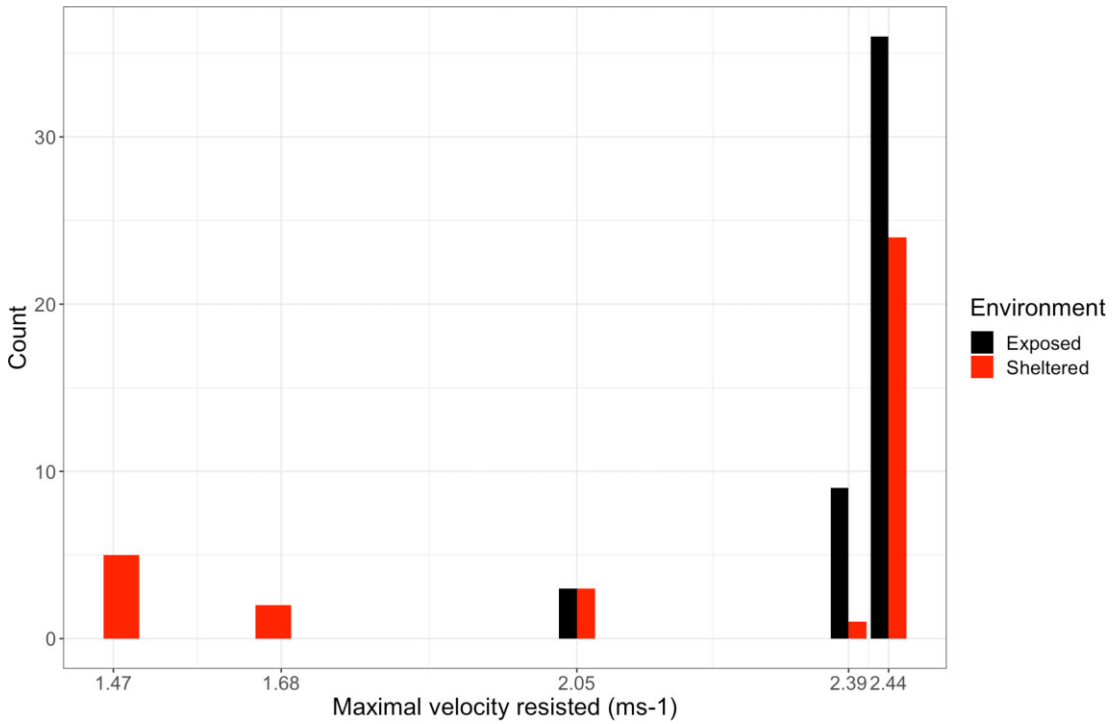

Figure 7. Number of individuals of *Fissurella latimarginata* from the two environment types in relation to the maximal water velocity resisted.

morphological heterogeneity independent of wave exposure (Fig. 6). Positive PC1 and PC2 scores are mostly correlated with shells having a peaked shape and a narrower and arched apertural margin, all characters typical of specimens inhabiting sheltered environments. In contrast, negative PC1 and PC2 scores are associated with shells having a more flattened shape and a wider and flatter aperture; such individuals tend to be the most predominant form in exposed environments. However, the CVA-based interspecific classification showed no differences between environments (overall classification accuracy = 56.9%) and sex (60.3%), and low classification efficiencies (Cohen's kappa was 0.138 and 0.125 for environment type and sex, respectively) (Table 1). Morphologically, females showed a more strongly defined lateral shell shape, when compared to males, with the overall classification accuracy being 85.1% and 26.5%, respectively.

Laboratory-controlled water flow experiments

Given the total shell length distribution analysed in the previous section (see Figs 3 and 4), individuals from both environments in the length range 50–65 mm L_s were selected for the trial in the water flume.

Limpets from sheltered areas became dislodged at the lowest free-stream velocity implemented in the experiments (1.48 m s^{-1}), while limpets from wave-exposed areas were dislodged from 2.05 m s^{-1} upwards (Fig. 7). Nonetheless, a high number of specimens ($n = 60$) from both coastal areas resisted the maximal velocity applied during the experiments (2.44 m s^{-1}) (Fig. 7). Among the limpets that remained attached after exposure to the highest flow velocity, 40% of them were collected from sheltered areas.

Given the absence of individuals from exposed areas dislodging at the lowest velocities of 1.47 and 1.68 m s^{-1} and the low number of individuals in general in the velocities 2.05 and 2.39 m s^{-1} (see Fig. 7), comparisons of the normalized variables and constant *a* between environments were performed only for the maximal velocity resisted (2.44 m s^{-1}). At the maximal velocity, the normalized variables (W_{si}: $t_{48} = 11.2$, $P < 0.001$; H_{li}: $t_{50.4} = 5.65$, $P < 0.001$; A_{fi}: $t_{63.1} = 3.90$, $P < 0.001$; L_{fi}: $t_{57.2} = 4.15$, $P < 0.001$; W_{fi}: $t_{52.5} = 2.92$, $P < 0.001$) showed higher values in wave-exposed habitats (Fig. 8).

The constant *a* showed a normal distribution (Exp.: $W = 0.97751$, $P = 0.6928$; Shl.: $W = 0.93808$, $P = 0.1209$). At the maximal velocity resisted (2.44 m s^{-1}), no significant differences were detected in the constant *a* between environments ($t_{46.713} = -0.93922$, $P = 0.352$; Fig. 9). Thus, the limpet's geometry, and fluid and flow properties were capable of predicting the detachment scenarios showing a strong correlation between the detachment velocity and the variables.

DISCUSSION

The present results support the hypothesis that populations of the limpet *Fissurella latimarginata* are characterized by different phenotypes in different environments, in this case habitats with differential wave exposure (i.e. sheltered *vs* exposed environments). Ecological studies indicate that in the intertidal zone molluscan morphological features, such as shell shape and body size, are modulated by the effect of wave energy (Trussell *et al.*, 1993; Denny & Blanchette, 2000), with higher mean total shell lengths and foot areas having been observed in gastropods living in exposed environments (Carvajal-Rodríguez *et al.*, 2005; Márquez *et al.*, 2015). The same trend was observed here for *F. latimarginata*, where limpets with wider shells, greater height and larger feet (i.e. in length, width and area) were found in more exposed areas. Our results indicate that for the studied species, greater attachment, as afforded by both a larger foot and wider shells, may be an effective strategy for resisting dislodgement by wave action. In sea snails, contrasting patterns were observed (Le Pennec *et al.*, 2017). Shorter shells are likely to provide greater access to protected cracks and crevices and are also likely to be associated with lower drag coefficients than larger shells (Trussell *et al.*, 1993; Carvajal-Rodríguez *et al.*, 2005). Among the traits crucial for the survival of molluscs in the hydrodynamic conditions characteristic of the intertidal zone are foot area, the lateral shape (i.e. compression) of the shell, the relative shell height

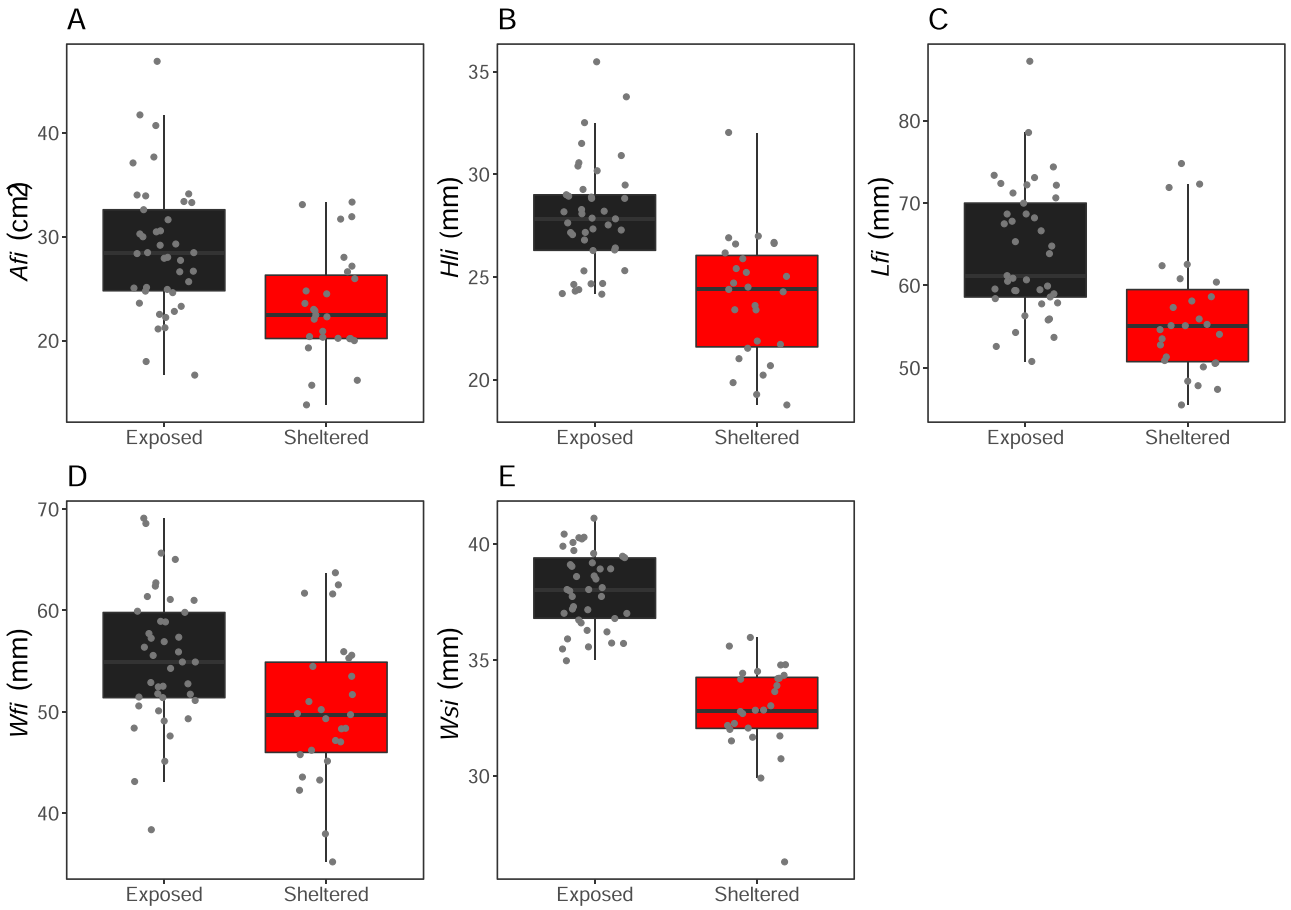

Figure 8. Variation in the five normalized variables at the maximal velocity resisted (2.44 m s^{-1}) for shores differentially exposed to wave energies. **A.** Foot area (A_{fi}, cm^2). **B.** Full limpet height (H_{li}, mm). **C.** Foot length (L_{fi}, mm). **D.** Foot width (W_{fi}, mm). **E.** Shell width (W_{si}, mm). Exposed environments are indicated by black shading and sheltered ones by red shading, with the horizontal lines within the boxes indicating the median. The dots represent the original data points.

and the outer shell apertural area (see Figs 5 and 6) (Trussell *et al.*, 1993; Le Pennec *et al.*, 2017). On a small scale, this segregation with respect to shell size offers ecological advantages, allowing intertidal molluscs to thrive across a range of contrasting habitats, resulting in the reduction of intraspecific competition (Livore *et al.*, 2018). This segregation has implications for physiology and survival, with compensatory processes in individuals from wave-swept habitats; these processes are evident from the variations in the energy allocated to growth or reproduction between individuals living in sheltered and exposed environments (Pulgar *et al.*, 2012). In specimens living in sheltered habitats, it is expected that maintenance costs will be low relative to those in specimens inhabiting exposed sites; an increase in foot weight has been observed in limpets from sheltered environments during winter and, although no effects on reproduction were observed, this increase in foot weight likely enables limpets to remain associated with the substrate (Pulgar *et al.*, 2012).

In the present work, *F. latimarginata* specimens from exposed environments present a round to laterally wider and posteriorly narrower shell shape with a relatively large aperture suitable for accommodating a larger foot needed to ensure attachment to the substrate. On the other hand, *F. latimarginata* specimens inhabiting protected coastal areas showed a more laterally compressed and posteriorly wider shell shape. Regarding the lateral view, the morphological variability found in the studied specimens did not allow us to differentiate between both environments nor between females and males. In this context, it is important to note that most of the morphometric studies on limpets are based on the dorsal view of the shell (Reisser, Marshall & Gardner, 2012; Carreira *et al.*, 2017; Faria *et al.*, 2017). In other geographic regions, limpets with a more pointed shape were reported on shores with higher insolation and thermal stress (Hines *et al.*, 2017), thus with less wave action. On the Ubatuba (Brazil) shores, the limpet *Lottia subrugosa* showed similar results to the present study for foot area, where limpets consistently showed a proportionally larger foot on exposed shores (Vieira & Bueno, 2019). Regarding full limpet height, our result is counterintuitive because one would expect a shift to lower heights in exposed environments. However, it should be noted that we measured the total height of the limpet and not the maximum height of the shell. The need to avoid dislodgment is probably the main factor affecting limpet height on the Chilean shores.

Similar patterns have been observed for *Littorina obtusata* and *Littorina saxatilis*, with individuals living in different conditions of wave exposure showing contrasting shell shape and body size (Trussell *et al.*, 1993; Boulding, Holst & Pilon, 1999; Trussell & Etter, 2001; Carvajal-Rodríguez *et al.*, 2005). Le Pennec *et al.* (2017), for example, have reported that a small and fragile 'wave ecotype' with a more globose shape was confined to wave-swept shores, whereas a large and robust 'crab ecotype' with a more elongated shape was found on less exposed shores. The presence of rounded shells with a wide aperture (more oval shape) in wave-exposed coastal areas may be due to physiological reasons, since larger muscles are needed to ensure attachment to the substrate in areas subject to harsh conditions (Goodrich, 1934; Wu, 1985; Trussell, 1997). In contrast, shells with a more conical shape may accommodate

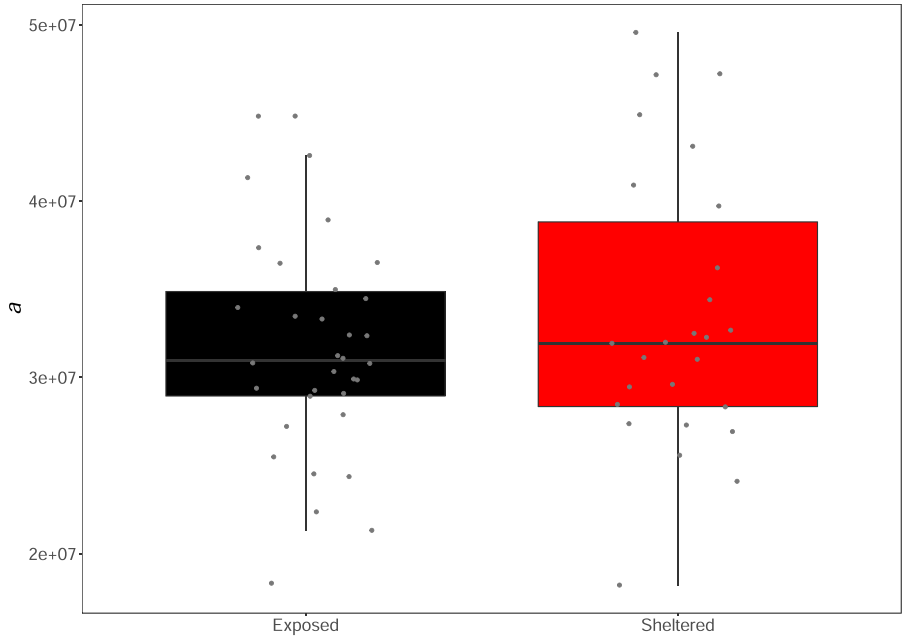

Figure 9. Variation in the constant *a* at the maximal velocity resisted (2.44 m s^{-1}) for shores differentially exposed to wave energies. Exposed habitats are indicated by black shading and sheltered environments by red shading, with the horizontal lines within the boxes indicating the median. The dots represent the original data points.

a larger body but a relatively smaller foot, an adaptation to sheltered environments, as has been shown in intertidal littorinids (Queiroga *et al.*, 2011).

Our results shed light on the direction and magnitude of phenotypic variability in *F. latimarginata* populations in relation to the resistance of individuals from both sheltered and exposed environments to dislodgement. Limpets from exposed environments were dislodged at higher velocities and these were associated with a laterally wider and posteriorly narrower shell, a shape that can accommodate a larger and wider foot and can thus make possible a larger contact area between the limpet and the substrate. In sheltered areas, limpets were dislodged at lower velocities, showing a lower resistance to wave action; our results show that these limpets were characterized by a more laterally compressed and peaked shape, and a smaller foot area that decreases the contact area with the substrate (i.e. to prevent water loss). Nonetheless, a high number of limpets from sheltered environments resisted the maximal velocity used in our study (2.44 m s^{-1}). This may be a consequence of the season when sampling was carried out. All the specimens used in the water flume experiments were collected in autumn and winter. As indicated previously, the foot weight in limpets from sheltered environments may increase during the winter (Pulgar *et al.*, 2012), thus increasing their resistance capacity to wave action. Although significant differences in A_{fi}, L_{fi} and W_{fi} were found between environments for the maximum velocity resisted, a clear overlap was observed (Fig. 8); this again is in agreement with foot weight increasing in the winter.

Our results show that *F. latimarginata* is locally adapted to the wave-swept conditions typical of exposed shores on the Chilean coast. Several traits, especially foot area and limpet full height, as well as the shell shape, are involved in the adaptation of this species to these environmental conditions. Interestingly, this study shows that limpets from sheltered habitats are resistant to high levels of wave action; this may be a consequence of possible morphological adaptations to compensate for the differences between environments. However, the evident difference in capacity to resist dislodgement was the most important factor separating the two habitats. As we have shown, the use of a flume-controlled hydrodynamic environment was useful to differentiate between individuals from the two habitats. The use of experiments based on channel water flows in studies on the shell phenotypic variability of marine molluscs constitutes a step forward in determining whether a phenotype is truly responding to hydrodynamic variations independent of other environmental factors potentially influencing the intertidal zone (Le Pennec *et al.*, 2017). The present study highlights the ability of *F. latimarginata* to resist harsh conditions regardless of the type of environment.

SUPPLEMENTARY MATERIAL

Supplementary material is available at *Journal of Molluscan Studies* online.

ACKNOWLEDGEMENTS

J.V. was supported by a grant from Fundação para a Ciência e Tecnologia (FCT; grant no. SFRH/BSAB/143056/2018) and D.C. by a grant from Dirección de Investigación de la Universidad Católica de la Santísima Concepción (UCSC; grant no. UCSC-DINREG 07/2018, Chile). This work was also funded by the Regional Government of Madeira (sabbatical leave). We are grateful to colleagues from UCSC for all their help with logistics and to the UCSC's Department of Civil Engineering, Faculty of Engineering for providing the hydraulic flume used in this work. Our special thanks to the technical staff at the Marine Biology Station of Lenga for their help with the collection of the specimens and subsequent maintenance in recirculating seawater tanks and to Carolina Leiva González for her crucial help with the flume experiments.

REFERENCES

ADAMS, D., COLLYER, M. & KALIONTZOPOULOU, A. 2018. Software for morphometric analyses. R package geomorph v. 3.0.7. Available at: https://cran.r-project.org/package=geomorph. Accessed 1 September 2018.

AGUIRRE, C., GARREAUD, R.D. & RUTLLANT, J.A. 2014. Surface ocean response to synoptic-scale variability in wind stress and heat

fluxes off south-central Chile. *Dynamics of Atmospheres and Oceans*, **65**, 64–85.

ANGELES, D.J., GOROSPE, J.G., TORRES, A.J. & DEMAYO, C.G. 2014. Length–weight relationship, body shape variation and asymmetry in body morphology of *Siganus guttatus* from selected areas in five Mindanao bays. *International Journal of Aquatic Science*, **5**: 40–57.

ATKINSON, W.D. & NEWBURY, S.F. 1984. The adaptations of the rough winkle, *Littorina rudis*, to desiccation and to dislodgement by wind and waves. *Journal of Animal Ecology*, **53**: 93–105.

BOOKSTEIN, F.L. 1997. *Morphometric tools for landmark data: geometry and biology*. Cambridge University Press, Cambridge.

BOULDING, E.G., HOLST, M. & PILON, V. 1999. Changes in selection on gastropod shell size and thickness with wave-exposure on northeastern Pacific shores. *Journal of Experimental Marine Biology and Ecology*, **232**: 217–239.

BOULDING, E.G. & Van ALSTYNE, K.L. 1993. Mechanisms of differential survival and growth of two species of *Littorina* on wave-exposed and on protected shores. *Journal of Experimental Marine Biology and Ecology*, **169**: 139–166.

BRETOS, M. 1988. Pesquería de lapas en Chile. *Medio Ambiente*, **9**: 7–12.

CARREIRA, G.P., SHAW, P.W., GONÇALVES, J.M. & McKEOWN, N.J. 2017. Congruent molecular and morphological diversity of Macaronesian limpets: insights into eco-evolutionary forces and tools for conservation. *Frontiers in Marine Science*, **4**: 75.

CARVAJAL-RODRÍGUEZ, A., CONDE-PADÍN, P. & ROLÁN-ALVAREZ, E. 2005. Decomposing shell form into size and shape by geometric morphometric methods in two sympatric ecotypes of *Littorina saxatilis*. *Journal of Molluscan Studies*, **71**: 313–318.

COLLAR, D. & WAINWRIGHT, P. 2009. Ecomorphology of centrarchid fishes. In: *Centrarchid fishes: diversity, biology and conservation* (S. Cooke & D. Philipp, eds), pp. 70–89. Wiley-Blackwell, West Sussex, UK.

DAHLHOFF, E.P., STILLMAN, J.H. & MENGE, B.A. 2002. Physiological community ecology: variation in metabolic activity of ecologically important rocky intertidal invertebrates along environmental gradients. *Integrative and Comparative Biology*, **42**: 862–871.

DENNY, M.W. & BLANCHETTE, C.A. 2000. Hydrodynamics, shell shape, behavior and survivorship in the owl limpet *Lottia gigantea*. *Journal of Experimental Biology*, **203**: 2623–2639.

DENNY, M.W. & GAINES, S.D. 1990. On the prediction of maximal intertidal wave forces. *Limnology and Oceanography*, **35**: 1–15.

De WOLF, H., BACKELJAU, T., MEDEIROS, R. & VERHAGEN, R. 1997. Microgeographical shell variation in *Littorina striata*, a planktonic developing periwinkle. *Marine Biology*, **129**: 331–342.

ETTER, R.J. 1988. Asymmetrical developmental plasticity in an intertidal snail. *Evolution: International Journal of Organic Evolution*, **42**: 322–334.

FARIA, J., MARTINS, G.M., PITA, A., RIBEIRO, P.A., HAWKINS, S.J., PRESA, P. & NETO, A.I. 2017. Disentangling the genetic and morphological structure of *Patella candei* complex in Macaronesia (NE Atlantic). *Ecology and Evolution*, **7**: 6125–6140.

FARRÉ, M., TUSET, V.M., CARTES, J.E., MASSUTÍ, E. & LOMBARTE, A. 2016. Depth-related trends in morphological and functional diversity of demersal fish assemblages in the western Mediterranean Sea. *Progress in Oceanography*, **147**: 22–37.

GOODRICH, C. 1934. *Studies of the gastropod family Pleuroceridae—I. Occasional papers of the Museum of Zoology, no. 286*. University of Michigan Press, Ann Arbor, MI.

GUNZ, P. & MITTEROECKER, P. 2013. Semilandmarks: a method for quantifying curves and surfaces. *Hystrix*, **24**: 103–109.

HAMMER, Ø., HARPER, D.A. & RYAN, P.D. 2001. PAST: paleontological statistics software package for education and data analysis. *Palaeontologia Electronica*, **4**: 1–9.

HARLEY, C.D., DENNY, M.W., MACH, K.J. & MILLER, L.P. 2009. Thermal stress and morphological adaptations in limpets. *Functional Ecology*, **23**: 292–301.

HELMUTH, B.S. & HOFMANN, G.E. 2001. Microhabitats, thermal heterogeneity, and patterns of physiological stress in the rocky intertidal zone. *Biological Bulletin*, **201**: 374–384.

HINES, H.N., MORRISS, H., SAUNDERS, K., WILLIAMS, R.L., YOUNG, S.L. & STAFFORD, R. 2017. Localized versus regional adaptation in limpet shell morphology across the Iberian Peninsula. *Marine Ecology*, **38**: e12472.

KEOUGH, M.J., QUINN, G.P. & BATHGATE, R. 1997. Geographic variation in interactions between size classes of the limpet *Cellana tramoserica*. *Journal of Experimental Marine Biology and Ecology*, **215**: 19–34.

KLINGENBERG, C.P. 2016. Size, shape, and form: concepts of allometry in geometric morphometrics. *Development Genes and Evolution*, **226**: 113–137.

LACHENBRUCH, P.A. & MICKEY, M.R. 1968. Estimation of error rates in discriminant analysis. *Technometrics*, **10**: 1–11.

Le PENNEC, G., BUTLIN, R.K., JONSSON, P.R., LARSSON, A.I., LINDBORG, J., BERGSTRÖM, E. & JOHANNESSON, K. 2017. Adaptation to dislodgement risk on wave-swept rocky shores in the snail *Littorina saxatilis*. *PLoS One*, **12**: e0186901.

LIVORE, J.P., MENDEZ, M.M., BIGATTI, G. & MÁRQUEZ, F. 2018. Habitat-modulated shell shape and spatial segregation in a Patagonian false limpet (*Siphonaria lessonii*). *Marine Ecology Progress Series*, **606**: 55–63.

LLEONART, J., SALAT, J. & TORRES, G.J. 2000. Removing allometric effects of body size in morphological analysis. *Journal of Theoretical Biology*, **205**: 85–93.

LOMBARTE, A. & LLEONART, J. 1993. Otolith size changes related with body growth, habitat depth and temperature. *Environmental Biology of Fishes*, **37**: 297–306.

MARDIA, K.V., KENT, J. & BIBBY, J. 1979. *Multivariate analysis*. Academic Press, Amsterdam.

MÁRQUEZ, F., ADAMI, M.L., TROVANT, B., NIETO-VILELA, R.A. & GONZÁLEZ-JOSÉ, R. 2018. Allometric differences on the shell shape of two scorched mussel species along the Atlantic South American Coast. *Evolutionary Ecology*, **32**: 43–56.

MÁRQUEZ, F., VILELA, R.A.N., LOZADA, M. & BIGATTI, G. 2015. Morphological and behavioral differences in the gastropod *Trophon geversianus* associated to distinct environmental conditions, as revealed by a multidisciplinary approach. *Journal of Sea Research*, **95**: 239–247.

MILLER, L.P., HARLEY, C.D. & DENNY, M.W. 2009. The role of temperature and desiccation stress in limiting the local-scale distribution of the owl limpet, *Lottia gigantea*. *Functional Ecology*, **23**: 756–767.

MITTEROECKER, P. & BOOKSTEIN, F. 2011. Linear discrimination, ordination, and the visualization of selection gradients in modern morphometrics. *Evolutionary Biology*, **38**: 100–114.

NAKIN, M.D.V. & McQUAID, C.D. 2014. Marine reserve effects on population density and size structure of commonly and rarely exploited limpets in South Africa. *African Journal of Marine Science*, **36**: 303–311.

NEWELL, R. 1979. *Biology of intertidal animals*. Edn 3. Marine Ecological Survey. Faversham, UK.

OLIVA, D. & CASTILLA, J.C. 1986. The effect of human exclusion on the population structure of key-hole limpets *Fissurella crassa* and *F. limbata* on the coast of central Chile. *Marine Ecology*, **7**: 201–217.

PROWSE, T.A.A. & PILE, A.J. 2005. Phenotypic homogeneity of two intertidal snails across a wave exposure gradient in South Australia. *Marine Biology Research*, **1**: 176–185.

PULGAR, J., ALVAREZ, M., DELGADILLO, A., HERRERA, I., BENITEZ, S., MORALES, J. & PULGAR, V. 2012. Impact of wave exposure on seasonal morphological and reproductive responses of the intertidal limpet *Fissurella crassa* (Mollusca: Archaegastropoda). *Journal of the Marine Biological Association of the United Kingdom*, **92**: 1595–1601.

QUEIROGA, H., COSTA, R., LEONARDO, N., SOARES, D. & CLEARY, D.F. 2011. Morphometric variation in two intertidal littorinid gastropods. *Contributions to Zoology*, **80**: 201–211.

R CORE TEAM. 2018. *R: a language and environment for statistical computing*. R Foundation for Statistical Computing, Vienna. Available at: https://www.R–project.org. Accessed 30 December 2018.

REISSER, C.M., MARSHALL, B.A. & GARDNER, J.P. 2012. A morphometric approach supporting genetic results in the taxonomy of the New Zealand limpets of the *Cellana strigilis* complex (Mollusca: Patellogastropoda: Nacellidae). *Invertebrate Systematics*, **26**: 193–203.

RIVADENEIRA, M.M., SANTORO, C.M. & MARQUET, P.A. 2010. Reconstructing the history of human impacts on coastal biodiversity

in Chile: constraints and opportunities. *Aquatic Conservation: Marine and Freshwater Ecosystems*, **20**: 74–82

ROHLF, F.J. 1999. Shape statistics: Procrustes superimpositions and tangent spaces. *Journal of Classification*, **16**: 197–223.

ROHLF, F.J. 2017a. *tpsDig version 2.30*. Department of Ecology & Evolution and Anthropology, State University of New York at Stony Brook, New York. Available at: http://www.sbmorphometrics.org/index.html. Accessed 15 September 2018.

ROHLF, F. 2017b. *tpsRelw version 1.67*. Department of Ecology & Evolution and Anthropology, State University of New York at Stony Brook, New York. Available at: http://www.sbmorphometrics.org/index.html. Accessed 15 September 2018.

ROHLF, F. 2017c. *tpsUtil version 1.69*. Department of Ecology & Evolution and Anthropology, State University of New York at Stony Brook, New York. Available at: http://www.sbmorphometrics.org/index.html. Accessed 15 September 2018.

ROHLF, F.J. & MARCUS, L.F. 1993. A revolution morphometrics. *Trends in Ecology & Evolution*, **8**: 129–132.

ROHLF, F.J. & SLICE, D. 1990. Extensions of the Procrustes method for the optimal superimposition of landmarks. *Systematic Biology*, **39**: 40–59.

SCHLAGER, S. 2017. Morpho and Rvcg—shape analysis in R: R-packages for geometric morphometrics, shape analysis and surface manipulations. In: *Statistical shape and deformation analysis* (G. Zheng, S. Li & G. Szekely, eds), pp. 217–256. Academic Press, Cambridge, MA.

SCHNEIDER, C.A., RASBAND, W.S. & ELICEIRI, K.W. 2012. NIH Image to ImageJ: 25 years of image analysis. *Nature Methods*, **9**: 671–675.

STRUB, P.T., JAMES, C., MONTECINO, V., RUTLLANT, J.A. & BLANCO, J.L. 2019. Ocean circulation along the southern Chile transition region (38–46°S): mean, seasonal and interannual variability, with a focus on 2014–2016. *Progress in Oceanography*, **172**: 159–198.

TRUCHOT, J.P. & DUHAMEL-JOUVE, A. 1980. Oxygen and carbon dioxide in the marine intertidal environment: diurnal and tidal changes in rockpools. *Respiration Physiology*, **39**: 241–254.

TRUSSELL, G.C. 1997. Phenotypic selection in an intertidal snail: effects of a catastrophic storm. *Marine Ecology Progress Series*, **151**: 73–79.

TRUSSELL, G.C. & ETTER, R.J. 2001. Integrating genetic and environmental forces that shape the evolution of geographic variation in a marine snail. *Genetica*, **112**: 321–337.

TRUSSELL, G.C., JOHNSON, A.S., RUDOLPH, S.G. & GILFILLAN, E.S. 1993. Resistance to dislodgement: habitat and size-specific differences in morphology and tenacity in an intertidal snail. *Marine Ecology Progress Series*, **100**: 135–144.

TUSET, V.M., LOMBARTE, A.G.J.A., GONZÁLEZ, J.A., PERTUSA, J.F. & LORENTE, M. 2003. Comparative morphology of the sagittal otolith in *Serranus* spp. *Journal of Fish Biology*, **63**: 1491–1504.

TUSET, V.M., OTERO-FERRER, J.L., GÓMEZ-ZURITA, J., VENERUS, L.A., STRANSKY, C., IMONDI, R., ORLOV, A.M., YE, Z., SANTSCHI, L., AFANASIEV, P.K., ZHUANG, L., FARRÉ, M., LOVE, M.S. & LOMBARTE, A. 2016. Otolith shape lends support to the sensory drive hypothesis in rockfishes. *Journal of Evolutionary Biology*, **29**: 2083–2097.

VASCONCELOS, J., SOUSA, R., TUSET, V.M. & RIERA, R. 2020. Island effect in the shell phenotypic plasticity of an intertidal gastropod. *Zoology*, **141**: 125802.

VIEIRA, E.A. & BUENO, M. 2019. Small spatial scale effects of wave action exposure on morphological traits of the limpet *Lottia subrugosa*. *Journal of the Marine Biological Association of the United Kingdom*, **99**: 1309–1315.

WU, S.K. 1985. The genus *Acanthina* (Gastropoda: Muricacea) in west America. *Special Publication of the Mukaishima Marine Biological Station*, **1985**: 45–66.

ZAR, J.H. 1996. *Biostatistical analysis*. Prentice Hall, Hoboken, NJ.